Direct Observation of Superconductivity in Calcium-Intercalated Bilayer Graphene by *in situ* Electrical Transport Measurements

S. Ichinokura[1,*], K. Sugawara[2], A. Takayama[1], T. Takahashi[2,3], and S. Hasegawa[1]
[1]*Department of Physics, University of Tokyo, 7-3-1 Hongo, Bunkyo-ku, Tokyo 113-0033, Japan*
[2]*WPI Research Center, Advanced Institute for Materials Research, Tohoku University, Sendai 980-8577, Japan and*
[3]*Department of Physics, Tohoku University, Sendai 980-8578, Japan*
(Dated: August 31, 2015)

We report the superconductivity in Ca-intercalated bilayer graphene C_6CaC_6, the thinnest limit of Ca graphite intercalation compound. We performed *in situ* electrical transport measurements on pristine bilayer graphene, C_6LiC_6 and C_6CaC_6 fabricated on SiC substrate under zero and non-zero magnetic field. While both bilayer graphene and C_6LiC_6 show non-superconducting behavior, C_6CaC_6 exhibits the superconductivity with transition temperature (T_c) of 4.0 K. The observed T_c in C_6CaC_6 and the absence of superconductivity in C_6LiC_6 show a good agreement with the theoretical prediction, suggesting the importance of a free-electron-like metallic band at the Fermi level to drive the superconductivity.

PACS numbers: 68.65.Pq, 72.80.Vp, 73.22.Pr, 74.70.Wz

Atomic-layer superconductors (ALSCs), where only one or a few atomic layers at the surfaces or interfaces become superconducting[1–8], have attracted considerable attentions owing to their two-dimensionallity[5–7] and possible existence of symmetry mixed Cooper pairs[9]. It is known that in ALSCs fabricated on semiconductor substrates, the superconducting-transition temperature (T_c) is in general suppressed in comparison with that of bulk[1–5] due to the interference from the substrate except for limited cases[7, 8]. In this sense, self-standing ALSCs free from the substrate effect have been desired to pursue higher T_c.

Graphene is a single atomic sheet of graphite and now a target of intensive theoretical and experimental studies because of its various peculiar but attractive properties such as the massless nature of carriers[10], the anomalous quantum Hall effect[10], the high carrier mobility to drive the ballistic transport[11], *etc.* Besides these superior properties, graphene has a very important inherent property, namely, self-standing crystal structure basically isolated from substrate. In this context, graphene is regarded as one of ideal materials to realize ALSCs free from the substrate effect. Just after the discovery of graphene[12], many intensive efforts have been made to fabricate superconducting graphene by intercalating metals like in graphite intercalation compounds (GICs). Ca-intercalated bilayer graphene (C_6CaC_6) is regarded as the most promising candidate because corresponding Ca-intercalated GIC (C_6Ca) has the highest T_c of 11.5 K among all GICs[13–16]. While some theoretical[17, 18] and spectroscopic[19] studies have proposed a similar electronic structure between C_6Ca[20–22] and C_6CaC_6, suggestive of superconductivity in C_6CaC_6, no direct evidences for superconductivity, such as superconducting gap and/or zero-resistance, have been reported. This may be mainly due to difficulty in handling reactive samples containing Ca, requiring an *in situ* measurement under ultrahigh vacuum at ultralow temperature[2–5].

In this Letter, we report on the observation of the zero-resistance state in C_6CaC_6 to directry prove the occurrence of superconduttivity by *in situ* electrical transport measurements. We compare the experimental results with those for pristine bilayer graphene and C_6LiC_6 as well as the theoretical predictions to obtain an insight into the superconducting property and mechanism in intercalated bilayer graphene.

To fabricate intercalated bilayer graphene [Fig. 1(a)], we at first prepared a high-quality pristine bilayer graphene sheet on a n-type Si rich 6H-SiC(0001) single crystal by heating the crystal up to 1550°C in an argon atmosphere[23]. After a short exposure to air, the grown bilayer graphene/SiC was transferred into a RHEED (reflection-high-energy electron diffraction) vacuum chamber where the transport measurements were also done. After heating the sample at 400°C for several hours in the chamber, we observed a RHEED pattern typical of clean bilayer graphene on SiC[Fig. 1(b)]. Then, we deposited Li atoms on the bilayer graphene sheet using a SAES Getter dispenser. The Li deposition produced several sharp $\sqrt{3} \times \sqrt{3}$ R30° spots in the RHEED pattern [pointed by yellow arrows in Fig.1(c)], indicating that Li atoms are intercalated in a regular manner between two adjacent graphene layers[24] as in bulk C_6Li. After confirming the growth of high-quality C_6LiC_6 on SiC, we then deposited Ca atoms on this C_6LiC_6 sheet to replace Li with Ca. During the Ca deposition, we kept the substrate at 150°C, slightly above the Li desorption temperature of 145°C. We observed that the Ca deposition transformed the $\sqrt{3} \times \sqrt{3}$ R30° spots into streaks [Fig. 1(d)], suggesting that intercalated Li atoms are replaced by Ca atoms[19]. Repeated cycles of Li and Ca deposition together with annealing at appropriate temperatures made the $\sqrt{3} \times \sqrt{3}$ R30° streaks brighter and brighter. Finally, we obtained the RHEED pattern in

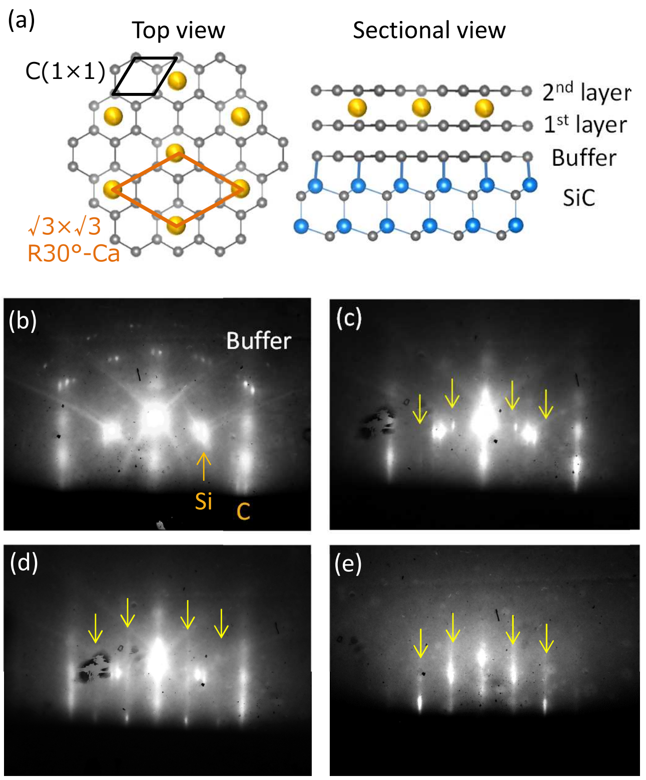

@

FIG. 1. (Color Online) (a) Crystal structure of C_6CaC_6 on SiC substrate. (b) RHEED pattern of pristine bilayer graphene. Si(1×1) spots from the substrate and C(1×1) spots from graphene are shown. Spots from the buffer layer with $6\sqrt{3}\times6\sqrt{3}$ R30° periodicity are also seen. (c) RHEED pattern of C_6LiC_6. (d), (e) Same for C_6CaC_6 (d) after the first Li-Ca replacing treatment and (e) after several cycles of the replacing treatments. Yellow allows indicate $\sqrt{3}\times\sqrt{3}$ R30° spots and streaks.

@ @

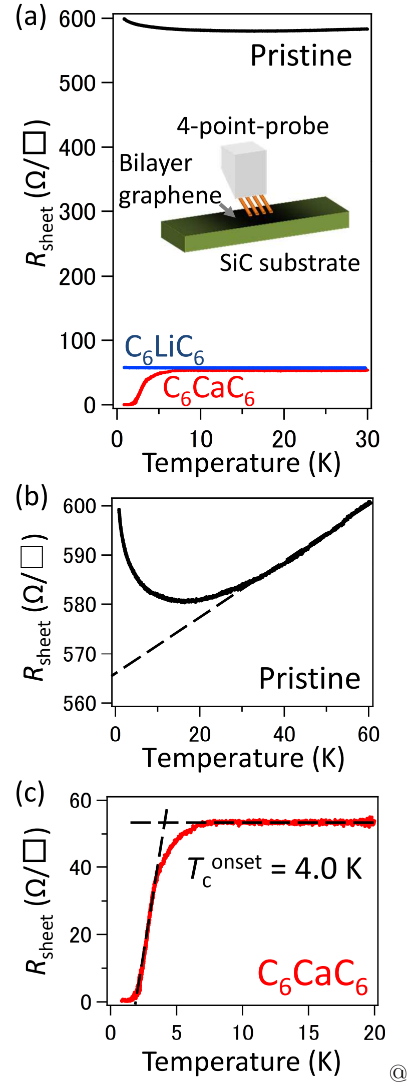

@

FIG. 2. (Color Online) (a) Sheet resistance R_{sheet} of pristine bilayer graphene, C_6LiC_6 and C_6CaC_6 as a function of temperature. Inset shows a schematic picture of 4-point-probe measurement set-up. (b) R_{sheet} of pristine bilayer graphene in an expanded scale from 0.8 to 60 K. Dashed line shows extrapolation toward 0 K. (c) R_{sheet} of C_6CaC_6 from 0.8 K to 20 K, showing $T_c^{\mathrm{onset}} = 4.0$ K and $T_c^{\mathrm{zero}} = 2.0$ K.

@ @

Fig. 1(e), where we observe sharp $\sqrt{3}\times\sqrt{3}$ R30° streaks, indicative of well-ordered C_6CaC_6.

After fabricating the sample as described above, we then transferred it on a stage for *in situ* electrical transport measurements with the 4-point-probe (4PP) method in the same vacuum chamber[25]. As shown in Fig. 2(a), the 4PP chip composed of four copper wires in 100 μm ϕ was contacted on the sample, and then cooled down to 0.8 K together with the sample. The results of temperature-dependent transport measurements on bilayer graphene, C_6LiC_6 and C_6CaC_6 are compared in Fig. 2(a). The sheet resistance (R_{sheet}) of pristine bilayer graphene shows a metallic character above 20 K, but turns into an insulating one at lower temperatures. This is usually observed in the transport characteristics of graphene and interpreted in terms of the localization effect due to the quantum interference[26–28]. The residual resistance at 0 K is estimated to be 565 Ω [Fig. 2(b)]. In C_6LiC_6 and C_6CaC_6, on the other hand, the R_{sheet} behaves as metallic, and their resistance is as low as ca. 10% of that of pristine bilayer graphene. This is because of the increase of the Fermi-surface volume by the career doping from Li or Ca atoms and the resultant folding of Brillouin zone due to the induced $\sqrt{3}\times\sqrt{3}$ R30° superstructure[19]. Importantly, the transition of R_{sheet} to zero-resistance is clearly seen at around 2 K in C_6CaC_6, which is the direct evidence of occurrence of superconductivity. It is also noteworthy that C_6LiC_6 does not show superconductivity down to 0.8 K, and instead exhibits a weak localization behavior as evident from a slight upturn in resistance at low temperature. Figure 2(c) shows the resistance of C_6CaC_6 at temperatures from 0.8 K to 20 K,

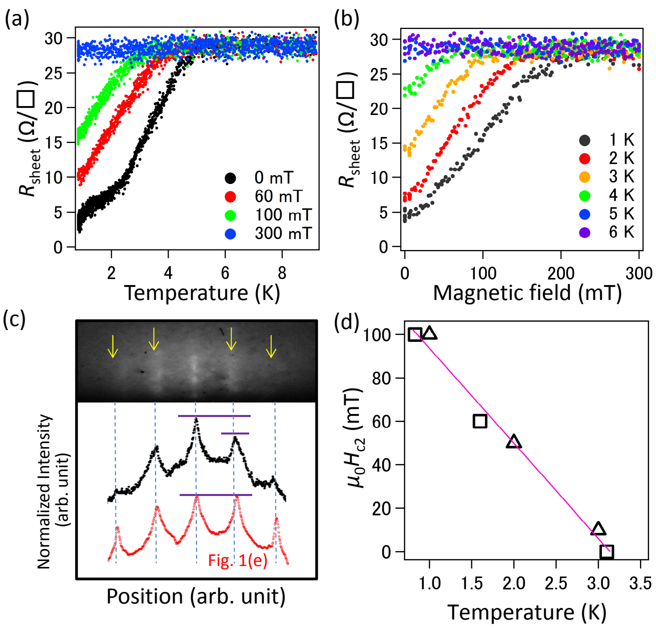

@

FIG. 3. (Color Online) (a) R_{sheet} of C_6CaC_6 as a function of temperature under different magnetic fields. (b) Same as (a) as a function of magnetic field for different temperatures. Magnetic field was applied perpendicular to the sample surface. (c) (Picture) RHEED pattern of this sample, showing weaker $\sqrt{3}\times\sqrt{3}$ R30° streaks than those in Fig. 1(e). Note that the sample is different from that in Fig. 1(e). (Plot) The intensity of RHEED pattern as a function of horizontal position for Fig. 3(c) (upper black dot) and Fig. 1(e) (lower red circle). The intensity is normalized by the peak height of central (1×1) streak. (d) Temperature dependence of the upper critical field $\mu_0 H_{c2}$ obtained from (a) (squares) and (b) (triangles). $\mu_0 H_{c2}$ is defined as the magnetic field where R_{sheet} drops to a half of normal-state resistance. Solid line shows the fitting based with the Ginzburg-Landau theory[40].

@ @

highlighting that R_{sheet} suddenly drops at around 4 K ($T_{\mathrm{c}}^{\mathrm{onset}} = 4.0$ K). One can also notice in Fig. 2(c) that R_{sheet} starts to decrease even above 4 K. This is probably due to the superconducting fluctuation inherent to low-dimensional superconductors[29].

To obtain further evidence for superconductivity, we conducted magnetoresistance measurements on another C_6CaC_6 sample prepared with a same method as described above. In the experiments, the magnetic field was applied perpendicular to the surface. Figures 3(a) and (b) show R_{sheet} data as a function of temperatures and magnetic fields. As seen in Fig. 3(a), the $T_{\mathrm{c}}^{\mathrm{onset}}$ gradually shifts to lower temperature as the magnetic field is increased. A similar behavior of $T_{\mathrm{c}}^{\mathrm{onset}}$ is also seen in Fig. 3(b). It is noted that the R_{sheet} curve did not fully drop to zero-resistance even at 0.8 K under zero magnetic field, suggesting that only a limited part of sample became superconducting and the superconducting paths were not fully connected between the current probes in this sample. In fact, as shown in Fig. 3(c), the $\sqrt{3}\times\sqrt{3}$ R30° streak originating in C_6CaC_6 is weaker in the present sample than in that of Fig. 1(e). This in return supports that the superconductivity emerges in the well-ordered $\sqrt{3}\times\sqrt{3}$ R30° superstructure. To see the temperature-dependence of the upper critical field ($\mu_0 H_{c2}$), we plot the magnitude of magnetic field at which the R_{sheet} is a half of the normal-state-resistance as a function of temperature in Fig. 3(d). We find that extracted points are well aligned linearly as seen in Fig. 3(d), indicating that these experimental results can be analyzed in the framework of the Ginzburg-Landau (GL) theory[30]. Numerical fittings with the GL theory show that the in-plane GL coherence length at zero Kelvin $\xi(0)$ is 49 ± 1 nm. This is comparable to or slightly larger than the in-plane $\xi(0)$ reported for bulk C_6Ca (29 – 36 nm)[13–16]. This shows a striking contrast with the case of usual ALSCs such as In on Si(111), where the $\xi(0) \sim 25$ nm[4] is much shorter than that of bulk (250 – 440 nm)[31]. This suggests the strong two-dimensional nature of superconductivity in both C_6CaC_6 and C_6Ca.

Now we discuss the origin of superconductivity in C_6CaC_6. While the T_{c} is lower than that of bulk C_6Ca (11.5 K), the present observation of superconductivity in C_6CaC_6 is striking. Because, no superconductivity has been observed so far in second-stage GICs ($C_{12}A$ where A is an alkali metal) which are a bulk analog of intercalated bilayer graphene (C_6AC_6). A simple estimation indicates that the carrier density in a single carbon layer in C_6CaC_6 should be reduced to a half of that in bulk C_6Ca. However, Mazin and Balatsky[17] have theoretically proposed the possibility of superconductivity in C_6CaC_6 despite the reduced carrier density, based on the similarity in the topology of Fermi surfaces consisting of a nearly-free electron band at the center of Brillouin zone and the π^* band at the zone boundary. They showed by calculations that the nearly-free electron band is partially occupied in C_6CaC_6 while it is totally unoccupied in C_6LiC_6, indicating the importance of the metallic nearly-free electron band for the superconductivity. This theoretical prediction shows a good agreement with the present observation that the superconductivity emerges in C_6CaC_6 while not in C_6LiC_6. Jishi *et al.*[18] have confirmed the band structure of intercalated bilayer graphene proposed by Mazin and Balatsky and further predicted the T_{c} of 4.7 K for C_6CaC_6. This shows a good quantitative agreement with the present observation of $T_{\mathrm{c}} = 4.0$ K. This strongly supports the theoretical proposal[17, 18] that the metallic nearly-free electron band at the center of Brillouin zone plays an essential role for the superconductivity. One may notice here that the calculations[17, 18] were done for ideal free-standing intercalated bilayer graphene while in reality the intercalated bilayer film is fabricated on SiC substrate, which may affect the electronic structure and consequently the superconductivity. In fact, a recent scanning tunnel microscope study reported that a charge density wave is

created at low temperatures in C_6CaC_6 on SiC due to the commensurate lattice matching[32]. It should be noted that despite these interferences from the substrate the T_c observed in C_6CaC_6 fabricated on SiC shows almost the same value as predicted for a free-standing C_6CaC_6, suggesting that the superconductivity in C_6CaC_6 is very robust.

In conclusion, we performed *in situ* electrical transport measurements on Ca-intercalated bilayer graphene C_6CaC_6 under zero and non-zero magnetic field. We have clearly observed that the resistance steeply drops at 4 K and reaches zero at 2 K under zero magnetic field, showing the occurrence of superconductivity with $T_c^{\rm onset} =$ 4.0 K and $T_c^{\rm zero} = 2.0$ K. The measurement under magnetic field has confirmed the superconductivity origin of the observed zero resistance. The observed $T_c^{\rm onset}$ is in good agreement with the theoretical prediction. The absence of superconductivity in pristine bilayer graphene and Li-intercalated bilayer graphene C_6LiC_6 in contrast to C_6CaC_6 suggests the importance of free-electron-like metallic band at the Fermi level to ignite the superconductivity.

We thank K. Suzuki and T. Sato at Tohoku University for their useful discussion. This work was supported by the JSPS (KAKENHI 15H02105, 25246025, 22246006) and the MEXT (Grant-in-Aid for Scientific Research on Innovative Areas "Science of Atomic Layers" 25107003 and "Molecular Architectonics" 25110010).

*Corresponding author:
ichinokura@surface.phys.s.u-tokyo.ac.jp

[1] S. Qin, J. Kim, Q. Niu, and C.-K. Shih, Science **324**, 1314 (2009).
[2] T. Zhang *et al.*, Nat. Phys. **6**, 104 (2010).
[3] T. Uchihashi, P. Mishra, M. Aono, and T. Nakayama, Phys. Rev Lett. **107**, 207001 (2011).
[4] M. Yamada, T. Hirahara, and S. Hasegawa, Phys. Rev. Lett. **110**, 237001 (2013).
[5] C. Brun *et al.*, Nat. Phys. **10**, 444 (2014).
[6] N. Reyren *et al.*, Science **317**, 1196 (2007).
[7] H.-M. Zhang *et al.*, Phys. Rev. Lett. **114**, 107003 (2015).
[8] J.-F. Ge, Z.-L. Liu, C. Liu, C.-L. Gao, D. Qian, Q.-K. Xue, Y. Liu, and J.-F. Jia, Nat. Mater. **14**, 285 (2015).
[9] L. P. Gor'kov and E. I. Rashba, Phys. Rev. Lett. **87**, 037004 (2001).
[10] K. Novoselov, A. K. Geim, S. Morozov, D. Jiang, M. Katsnelson, I. Grigorieva, S. Dubonos, and A. Firsov, Nature **438**, 197 (2005).
[11] K. S. Novoselov, Z. Jiang, Y. Zhang, S. Morozov, H. Stormer, U. Zeitler, J. Maan, G. Boebinger, P. Kim, and A. Geim, Science **315**, 1379 (2007).
[12] K. S. Novoselov, A. K. Geim, S. Morozov, D. Jiang, Y. Zhang, S. Dubonos, I. Grigorieva, and A. Firsov, Science **306**, 666 (2004).
[13] T. E. Weller, M. Ellerby, S. S. Saxena, R. P. Smith, and N. T. Skipper, Nat. Phys. **1**, 39 (2005).
[14] N. Emery, C. Hérold, M. d'Astuto, V. Garcia, C. Bellin, J. F. Marêché, P. Lagrange, and G. Loupias, Phys. Rev. Lett. **95**, 087003 (2005).
[15] E. Jobiliong, H. D. Zhou, J. A. Janik, Y.-J. Jo, L. Balicas, J. S. Brooks, and C. R. Wiebe, Phys. Rev. B **76**, 052511 (2007).
[16] R. Xie, D. Rosenmann, A. Rydh, H. Claus, G. Karapetrov, W. Kwok, and U. Welp, Physica C: Superconductivity **439**, 43 (2006).
[17] I. Mazin and A. Balatsky, Phil. Mag. Lett. **90**, 731 (2010).
[18] R. Jishi, D. Guzman, and H. Alyahyaei, Adv. Studies Theor. Phys. **5**, 703 (2011).
[19] K. Kanetani, K. Sugawara, T. Sato, R. Shimizu, K. Iwaya, T. Hitosugi, and T. Takahashi, Proc. Natl. Acad. Sci. USA **109**, 19610 (2012).
[20] G. Csányi, P. Littlewood, A. H. Nevidomskyy, C. J. Pickard, and B. Simons, Nat. Phys. **1**, 42 (2005).
[21] K. Sugawara, T. Sato, and T. Takahashi, Nat. Phys. **5**, 40 (2009).
[22] S.-L. Yang, J. Sobota, C. Howard, C. Pickard, M. Hashimoto, D. Lu, S.-K. Mo, P. Kirchmann, and Z.-X. Shen, Nat. Commun. **5** (2014).
[23] K. Sugawara, T. Sato, K. Kanetani, and T. Takahashi, J. Phys. Soc. Jpn. **80**, 024705 (2011).
[24] K. Sugawara, K. Kanetani, T. Sato, and T. Takahashi, AIP Adv. **1**, 022103 (2011).
[25] M. Yamada, T. Hirahara, R. Hobara, S. Hasegawa, H. Mizuno, Y. Miyatake, and T. Nagamura, e-J. Surf. Sci. Nanotech. **10**, 400 (2012).
[26] X. Wu, X. Li, Z. Song, C. Berger, and W. A. de Heer, Phys. Rev. Lett. **98**, 136801 (2007).
[27] F. V. Tikhonenko, D. W. Horsell, R. V. Gorbachev, and A. K. Savchenko, Phys. Rev. Lett. **100**, 056802 (2008).
[28] Y.-F. Chen, M.-H. Bae, C. Chialvo, T. Dirks, A. Bezryadin, and N. Mason, J. Phys.: Condens. Matter **22**, 205301 (2010).
[29] L. Aslamasov and A. Larkin, Phys. Lett. A **26**, 238 (1968).
[30] M. Tinkham, *Introduction to superconductivity* (Courier Corporation, 2012).
[31] R. D. Chaudhari and J. B. Brown, Phys. Rev. **139**, A1482 (1965).
[32] R. Shimizu, K. Sugawara, K. Kanetani, K. Iwaya, T. Sato, T. Takahashi, and T. Hitosugi, Phys. Rev. Lett. **114**, 146103 (2015).